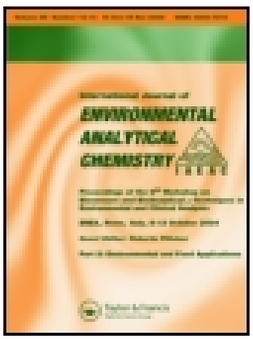

International Journal of Environmental Analytical Chemistry

ISSN: 0306-7319 (Print) 1029-0397 (Online) Journal homepage: https://www.tandfonline.com/loi/geac20

A novel approach in adsorption of heavy metal ions from aqueous solution using synthesized MCM-41 from coal bottom ash

Dinh-Hieu Vu, Hoang-Bac Bui, Xuan-Nam Bui, Dinh An-Nguyen, Qui-Thao Le, Ngoc-Hoan Do & Hoang Nguyen

To cite this article: Dinh-Hieu Vu, Hoang-Bac Bui, Xuan-Nam Bui, Dinh An-Nguyen, Qui-Thao Le, Ngoc-Hoan Do & Hoang Nguyen (2019): A novel approach in adsorption of heavy metal ions from aqueous solution using synthesized MCM-41 from coal bottom ash, International Journal of Environmental Analytical Chemistry

To link to this article: https://doi.org/10.1080/03067319.2019.1651300

Published online: 08 Aug 2019.

INTERNATIONAL JOURNAL OF ENVIRONMENTAL ANALYTICAL CHEMISTRY
https://doi.org/10.1080/03067319.2019.1651300

Taylor & Francis
Taylor & Francis Group

ARTICLE

A novel approach in adsorption of heavy metal ions from aqueous solution using synthesized MCM-41 from coal bottom ash

Dinh-Hieu Vu[a], Hoang-Bac Bui[b,c], Xuan-Nam Bui[a,d], Dinh An-Nguyen[a], Qui-Thao Le[a,d], Ngoc-Hoan Do[a,e] and Hoang Nguyen[f]

[a]Department of Surface Mining, Mining Faculty, Hanoi University of Mining and Geology, Hanoi, Vietnam; [b]Faculty of Geosciences and Geoengineering, Hanoi University of Mining and Geology, Hanoi, Vietnam; [c]Center for Excellence in Analysis and Experiment, Hanoi University of Mining and Geology, Hanoi, Vietnam; [d]Center for Mining, Electro-Mechanical Research, Hanoi University of Mining and Geology, Hanoi, Vietnam; [e]Faculty of Mining, Saint-Petersburg Mining University, Saint-Petersburg, Russia; [f]Institute of Research and Development, Duy Tan University, Da Nang 550000, Vietnam

ABSTRACT

In this study, mesoporous molecular sieve (MCM-41) was successfully synthesized from coal bottom ash (CBA). Different ratios of sodium hydroxide and CBA, as well as various calcination temperatures in alkali synthesis, were studied carefully to determine the optimum conditions for extracting silica from CBA powder. The synthesized products were characterized by X-ray diffraction (XRD), Fourier-transform infrared spectroscopy (FTIR), solid-state nuclear magnetic resonance (NMR), adsorption-desorption N_2, scanning electron microscope (SEM), and transmission electron microscopy (TEM). The results show that the best CBA -synthesized MCM-41 has a specific surface area of 932 m^2/g, a pore volume of 0.93 cm^3/g and a pore diameter of 3.14 nm. Finally, the effect of removing heavy metals (Pb^{2+}, Cu^{2+}, and Cd^{2+}) from the aqueous solution of the best CBA -synthesized MCM-41 was also determined at the optimum conditions obtained as 25°C, pH = 5 and reaction time of 12 hours. The MCM-41 required to achieve maximum heavy metal removal was found to be 1.67 g/l with the removal efficiencies of 99.4%, 41.66%, and 43.98% for Pb^{2+}, Cu^{2+} and Cd^{2+}, respectively. Moreover, the intrinsic parameters of Langmuir and Freundlich adsorption isotherms were obtained by fitting experimental data. The experimental results revealed that the MCM-41 could be used as an executable and inexpensive adsorbent for the removal of heavy metal ions from aqueous solution

ARTICLE HISTORY
Received 28 May 2019
Accepted 8 July 2019

KEYWORDS
MCM-41; heavy metal; adsorption isotherms; coal bottom ash; synthesis

1. Introduction

Coal bottom ash is a part of the non-combustible residue of a coal furnace. CBA primarily consists of silica, alumina, calcium oxide and iron with the physical characteristics of silty-sandy material [1–3]. Efficient disposal of CBA is an important problem on economic and environmental implications, and converting CBA into useful materials is

CONTACT Dinh-Hieu Vu vudinhhieu@humg.edu.vn; Hoang Nguyen nguyenhoang23@duytan.edu.vn

one of the common ways. CBA was primarily recycled in civil engineering applications such as cement productions, construction material, and road construction [4]. To date, there have been several studies in the conversion of CBA to form new materials. Researches have reported on the production of ceramic [5], humidity control material [5,6], adsorbent [7,8], pyrolysis [9,10], and the effects of adding CBA to cement mortar [11,12], and Portland cement in concrete [13,14]. Presently, despite the increasing interest in using BA as a raw material but the proper studies have not been done to reuse of CBA as a silica source for the synthesis of mesoporous silica materials.

On the other hand, mesoporous materials (MCM-41) with advanced porous functionalities of uniform pore sizes, large surface area, and connectivity have found many applications such as purification, catalysts, adsorbents, supports, electronic and sensing devices, drug delivery agents [15,16], and humidity controlling [17,18]. MCM-41 was also used to absorb volatile organic compounds (VOCs) from air, nitrobenzene, phenol, chlorophenol and metal cations from wastewater [19]. Mesoporous MCM-41 material has been synthesized from various silica precursors, including fumed silica, sodium silicate, *n*-alkoxysilanes, *n*-alkylamines, TEOS (tetraethylorthosilicate), and aerosol [20,21]. However, the economic costs for the industrial production of these precursors are high due to the cost of the initial material. The industrial-scale production of MCM-41 is likely to be economically restrictive if silica source, in particular, is selected [22,23]. Various research studies have been reported on the preparation of mesoporous MCM-41 material from the cheap silica source reusing from municipal waste, such as coal fly ash (CFA) [24,25], plant CFA [15], and volclay [26,27]. Most studies in the synthesis of mesoporous molecular sieve material from recycling ash as the silica precursors are based on the alkaline hydrothermal method [28–31]. Also, the combination of alkali-metal hydroxide with aluminosilicates is known to be a common technique to dissolve Al, Si, and some metallic species (e.g. for chemical analysis forming silica precursors). Then, MCM-41 product can be produced with a high Si/Al molar ratio of silica precursor using cetyltrimethylammonium bromide (CTAB) [24,32], cetyltrimethylammonium chloride (CTACl) [33], and cetyltrimethylammonium hydroxide (CTMAOH) as the surfactants [22].

In recent years, due to economic development needs and environmental concerns, the removal of heavy metal from waste effluents has been extensively studied. The removal of heavy metal is done through various methods such as solvent extraction, chemical precipitation, ion-exchange, adsorption or reverse osmosis. The adsorption among these processes is a practical method with a widespread use because it is convenient and economical, and has a high level of efficiency for the removal of heavy metals from wastewater as an effective technique [34–36]. Absorption is superior to other water treatment methods because of its initial cost, simplicity of design, simplicity of operation, and lack of sensitivity to toxic compounds [37,38].

The use of materials with surface functional groups, such as MCM-41 or MCM-48 for the removal of heavy metals in wastewater shows improved selectivity [39,40]. MCM-41 was used to remove the cationic nitrobenzene, o-chlorophenol, phenol, and divalent cations from wastewater [40,41], volatile organic compounds (VOCs) from indoor air [42], absorb heavy metals [43] and adsorb anionic [44]. However, literature studies on the effectiveness of removal of functional MCM-41 for Pb^{2+}, Cu^{2+}, and Cd^{2+} are very limited.

This study presents a methodology to generate silica precursor from CBA for production of the MCM-41 materials by applying the alkaline-fused hydrothermal process. The influences of initial material ratios (NaOH, CBA) and calcining temperature on the alkali fusion process were investigated to determine the best alkali-fused CBA powders. The effect of the deionized water ratios to achieve the highest Si/Al ratio in a precursor solution for synthesis of the MCM-41 products was also studied. The properties of products are tested through various techniques such as ICP-AES, XRD, FTIR, NMR, N_2 adsorption of solid state desorption, SEM and TEM. The best product (MCM-41) was created to test the ability to absorb heavy metals (Pb^{2+}, Cu^{2+}, and Cd^{2+}) from aqueous solution.

2. Experimental

2.1. Preparation of raw materials

The coal bottom ash used in the batch experiments was collected from Uong Bi Thermal Power Plant at Uong Bi City, Quang Ninh Province, Vietnam. The loss on ignition (LOI) of the dry sample was determined by heating a pre-weighed to 800 °C for two hours. The CBA material was then pulverized with a ball mill until they could pass through a 75 µm sieve to obtain a fine powder [45]. The dried and homogenized CBA powder was then stored in a desiccator until testing.

2.2. Synthesis of MCM-41

The synthesis of the MCM-41 product from CBA included two main steps: the extraction of silica from the CBA and the synthesis of MCM-41 from silica precursor. For the extraction of silica (in the form of sodium silicate), the alkali fusion method was adopted in this study. The fusion process was carried out by mixing sodium hydroxide and CBA powder (NaOH: CBA) at ratios of 1:1, 1.25:1, and 1.5:1. The mixtures were heated in an oven at 300 °C, 400 °C, 500 °C, and 600 °C for several hours to obtain the consolidated volumes; then, they were cooled at room temperature. The best alkali-fused CBA powders determined with the maximum of extraction yield SiO_2 were mixed with deionized water in weight ratios of Liquid/Solid (L/S) = 3, 5, and 7 (Table 2) and aged for one day at 25 °C to form three solutions, respectively. The concentrations of Al, Si, and Na in the supernatants were measured to calculate the Si/Al ratio. The solutions were subsequently filtered to obtain three supernatants.

During a typical MCM-41 synthesis stage, cetyltrimethylammonium bromide (CTAB) was dissolved in deionized water at 25 °C, then sodium silicates as the source of silica from three supernatants of the alkali-fused CBA powder were slowly added to form three aqueous micellar solutions. The mixture was agitated with a mechanical shaker at (25 ± 2 °C) for 1 h at pH of 10 and then hydrothermally treated for 2 days at 100 °C in which the pH values were adjusted to about 7–8. Then the resulting solids were filtered and washed using deionized water later dried overnight at 105 °C. Finally, the materials were calcined at 550 °C for 10 hours to obtain three mesoporous MCM-41 materials (M3, M5, and M7). For comparison, the siliceous MCM-41 was synthesized by using pure

chemicals for manufacturing an MS sample following the procedure reported by Ryoo and Kim [46].

2.3. Heavy metals adsorption experiments

The stock solutions were prepared by dissolving analytical grade nitrate salts of Pb^{2+}, Cu^{2+}, and Cd^{2+} at a concentration of 100 mg/l in deionized water. The working solutions were prepared by diluting the stock solution in deionized water and using 1M NaOH to control the pH of each solution at 5. All the adsorption experiments were done on an orbital shaker (200 rpm) using conical flasks at ambient temperature. In all tests, 50 mg of MCM-41 was thoroughly mixed into 30 ml of a single metal or mixture solutions at 25°C for 24 hours. After that, the solution with a syringe filter (0.20 m) was filtered to collect the final solutions. The concentration of the respective metal in the filtrate was measured by ICP-AES.

2.4. Characterization

The characteristics of MCM-41 samples were confirmed by using various techniques. Single-crystal X-rays diffraction (XRD) study was performed with an X'Pert PRO diffractometer equipped with a Cu K radiation. The chemical compositions were analyzed by using ICP-AES. Scanning electron micrographs (SEM) was recorded using an XL30 ESEM Philips. Infrared spectra were measured on a JEOL JIR-7000, Fourier transforms spectrometer in the frequency range of 400–4000 cm^{-1}. Both FTIR and SEM analyses were done on the coal bottom ash samples to find changes in the functional groups and morphology. Transmission electron microscopy (TEM) was determined with a JEOL 2010. Pore size distributions were determined according to the Barrett–Joyner–Halenda (BJH) algorithm. The specific surface area was confirmed by nitrogen adsorption using SA3100, according to the Brunauer–Emmett–Teller (BET) method. Solid-state Si and Al NMR spectra were measured with a Varian VXP-400. The metal ion absorption capacity of the material was explained by Langmuir and Freundlich isothermal theory.

3. Results and discussion

3.1. The extraction of si from the coal bottom ash and synthesis MCM-41

The results obtained from the preliminary analysis of chemical composition and amorphous phases of CBA are shown in Table 1 and Figure 1. The results reveal that the chemical compositions of CBA are SiO_2 as quartz (54.97%), Al_2O_3 (14.61%), and Fe_2O_3 (7.59%). Besides that, there are small amounts of oxides of Mg, Ca, K, Ti, P in the CBA [47]. The leaching concentration of heavy metals, derived from the TCLP test, was also shown in Table 1. From the values reported, it can be concluded that the concentration of heavy metals in the samples was lower than the limits set by the US-EPA [48]. Some agglomerates of particles with small spherical particles along are seen in the image. In general, CBA is safe and potential raw material to extract silica for preparing mesoporous molecular sieves.

Table 1. Chemical compositions and TCLP results of the CBA.

Chemical composition (wt.%)		TCLP results (mg/l)		
Component	Values	Component	Values	Regulatory*
SiO_2	54.97	Cd	0.23	1
Al_2O_3	14.61	Pb	0.1	5
Na_2O	1.07	Zn	11.2	-
K_2O	2.98	Cr	0.27	5
MgO	2.31	Cu	3.12	15
CaO	5.12			
TiO_2	0.84			
Fe_2O_3	7.59			
P_2O_5	5.38			

Regulatory*: From United State Environmental Protection Agency (US-EPA)

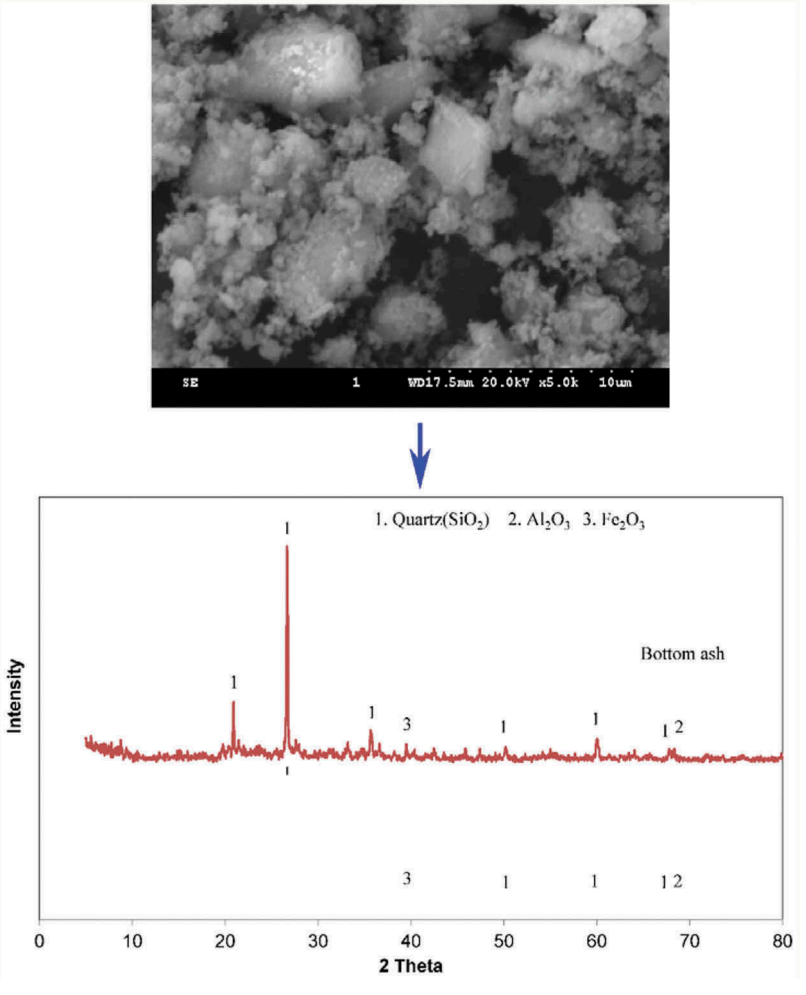

Figure 1. XRD and SEM results of CBA.

To release silica, the CBA was fused with sodium hydroxide at three ratios of NaOH/CBA = 1.0, 1.25, and 1.5, and the produced solid substances were then heated in an oven at 300°C, 400°C, 500 °C, and 600 °C for several hours to obtain a consolidated mass,

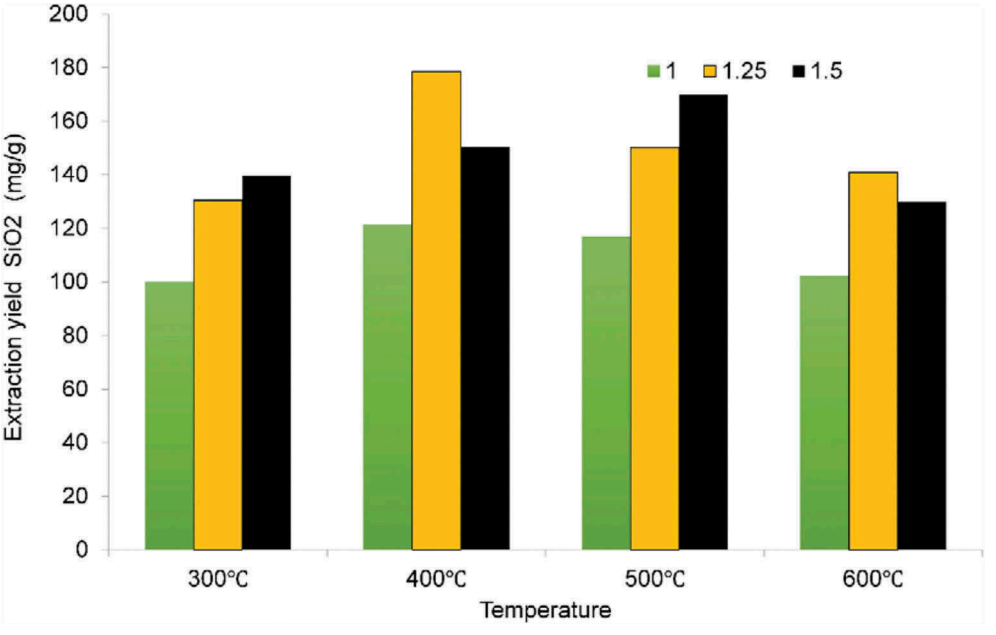

Figure 2. Extraction yield SiO_2 from CBA.

cooled to room temperature and grounded overnight as discussed in Section 2.2. Figure 2 provides the effects of heating temperature and NaOH/CBA ratio on the sodium silicate formation [47]. The result indicated that the mixture formed with the NaOH/CBA ratio of 1.25 and the heating temperature of 400 °C shows the maximum of extraction yield SiO_2 (178 mg/g). Also, the XRD diffraction pattern from Figure 3 confirmed that quartz was completely converted into sodium silicate (Na_2SiO_3) and little nepheline ($NaAlSiO_4$). The result from Figure 3 indicates that the crystalline silica in its natural reaction with sodium hydroxide to create sodium silicate dissolved in the fusion process. Therefore, it can be deduced that the extraction of silica from mullite and quartz into sodium silicate has been successful through fusion, and this process produces a cheap silica source to create mesoporous silica MCM-41. Therefore, the experimental conditions for alkali-fused CBA powders that exhibit the best extraction of Si are the NaOH/CBA ratio of 1.25 and the heating temperature of 400 °C.

The best alkali-fused CBA powders were mixed with deionized water in weight ratios of Liquid/Solid (L/S) = 3, 5, and 7 (Table 2) and aged for one day at 25 °C to form three supernatants. Table 2 presents the Si concentration ranging from 4100 ± 290 mg/l (L/S = 7) to 11300 ± 470 mg/l (L/S = 3), the Al concentration ranging from 80 ± 9 mg/l (L/S = 7) to 520 ± 62 mg/l (L/S = 3). For Na, the lowest and highest concentrations were found in extracts at L/S = 7 (48500 ± 3000 mg/l) and L/S = 3 (93000 ± 5700 mg/l), respectively. This also agrees with some earlier observations, which showed that the high N ion concentration in the precursor solution was known to interfere with the formation of the MCM-41 phase [27]. These findings suggest that in general, the chemical concentrations of solution increase as L/S ratio decreases. However, the highest Si/Al ratio (Si/Al = 51) was found for extract in solution with L/S = 7, and the lowest

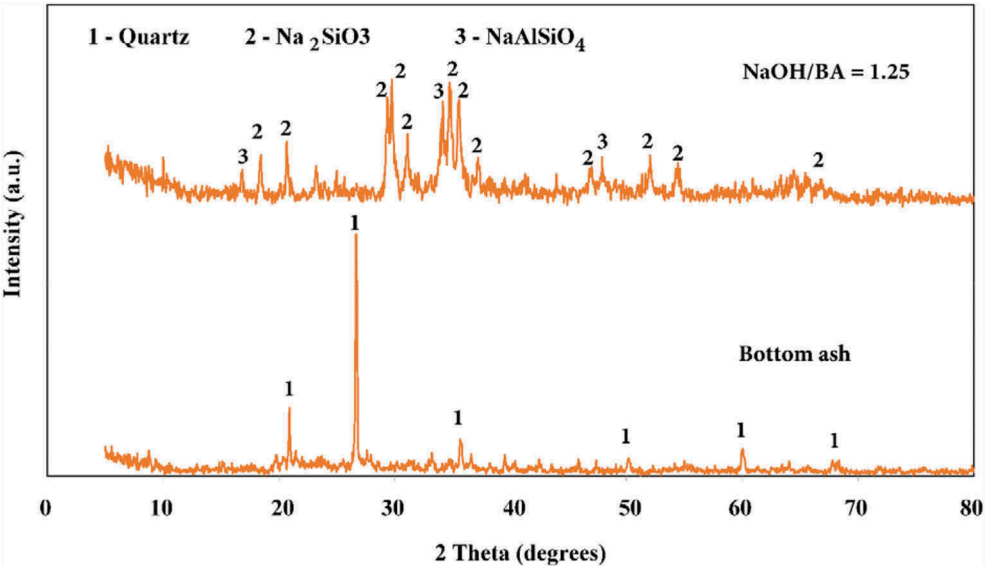

Figure 3. XRD results of the best alkali-fused CBA (NaOH/CBA = 1.25; 400 °C).

Table 2. Concentrations of Si, Al, Na, and Fe in the supernatants (mg/l).

L/Sa	Si	Al	Na	Fe	Si/Al
3	11300 ± 470	520 ± 62	93000 ± 5700	5.33 ± 0.47	22
5	8000 ± 270	420 ± 16	66000 ± 2400	1 ± 0	19
7	4100 ± 290	80 ± 9	48500 ± 3000	0.33 ± 0.47	51

aL – The deionized water and S – The best alkali-fused CBA powder

Si/Al ratio (Si/Al = 19) was found for extract in solution with L/S = 5. The Si/Al values of MCM-41 are high in comparison with the Si/Al = 3,7 in bottom ash and other mesoporous materials fabricated from CFA as well as Polish fly ashes [32].

3.2. Characteristics of MCM-41

Table 3 provides the main chemical composition of MCM-41 products. As can be viewed from this table, the SiO_2 content of M7 sample is higher than that of M3 and M5 samples

Table 3. The chemical composition of MCM-41 products (wt.%).

	Chemical composition					
Sample	SiO_2	Al_2O_3	Na_2O	K_2O	CaO	Fe_2O_3
M3	91.81	5.11	1.47	0.49	0.15	0.6
M5	91.22	5.21	2.93	0.57	N.D	0.33
M7	94.72	3.22	1.63	0.26	N.D	0.13
MS	98.20	N.D	N.D	N.D	N.D	N.D

N.D: No Detection

and also more closely with that of MS samples. In general, the SiO_2 compositions in all of the CBA-synthesized MCM-41 samples are higher than 90%, confirming that CBA can be used successfully to prepare MCM-41 through a relatively simple process involving alkali fusion.

Figure 4 provides the results obtained from a preliminary analysis of X-ray diffraction. As can be seen from Figure 4, the strong peak (100) in CBA-synthesized MCM-41 (M3, M5, and M7 samples) is recognized as the peak characteristic of the MCM-41 family (MS sample). Also, two peaks (110) and (200) indicate an effective appearance of 2-dimensional hexagonal structure in the samples.

From the XRD patterns of the adsorbents, the primary crystalline species in the coal bottom ash sample were quartz (SiO_2) and mullite ($3Al_2O_3 \cdot 2SiO_2$) as identified by the sharp peaks, while the presence of the amorphous phases of SiO_2 were identified by the presence of a broad diffraction peak (near $2\theta = 24^{\circ}$). The results of X-ray diffraction data matched the results of the study and showed that MCM-41 was successfully prepared from CBA.

Figure 5 shows the morphology of the various MCM-41products. It can be seen that the CBA -synthesized MCM-41 (M3, M5, and M7) exhibited mainly agglomerations of non-morphology with particles sizes around 1.5 μm and the L/S ratio increase as the porosity increase. This study produced results which corroborate the finding of some previous studies in this field [49–51]. By contrast, the morphology of the samples show the hexagonal morphological and fine spherical particles with a diameter of approximately 1.5μm and smaller than MCM-41 sample (MS) which was prepared from pure silica. The morphology of silica extracts showed high porosity, which confirmed excellent absorption capacity of MCM-41 samples.

The TEM images at 539.85 °C (813 K) present impurities as well as on the inner surface of the MCM-41 synthesize the CBA pore from the TEM image (Figure 6).

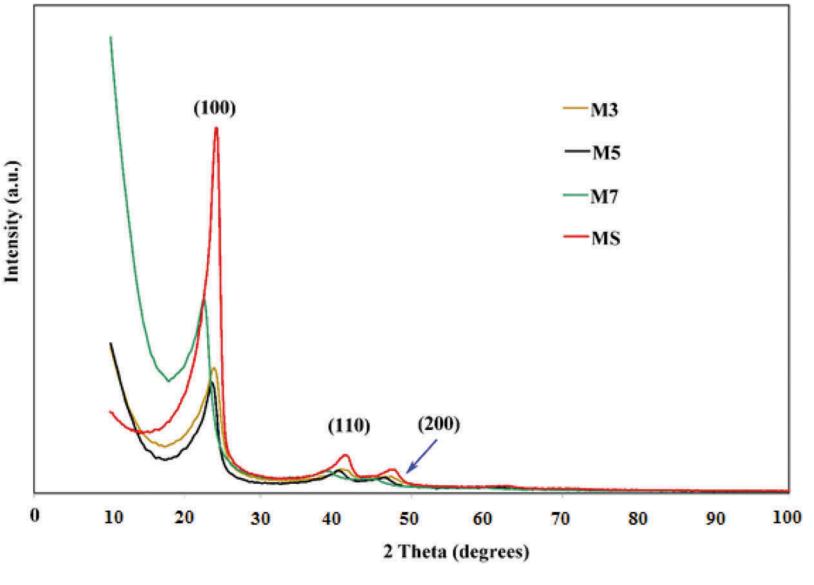

Figure 4. XRD results of MCM-41products.

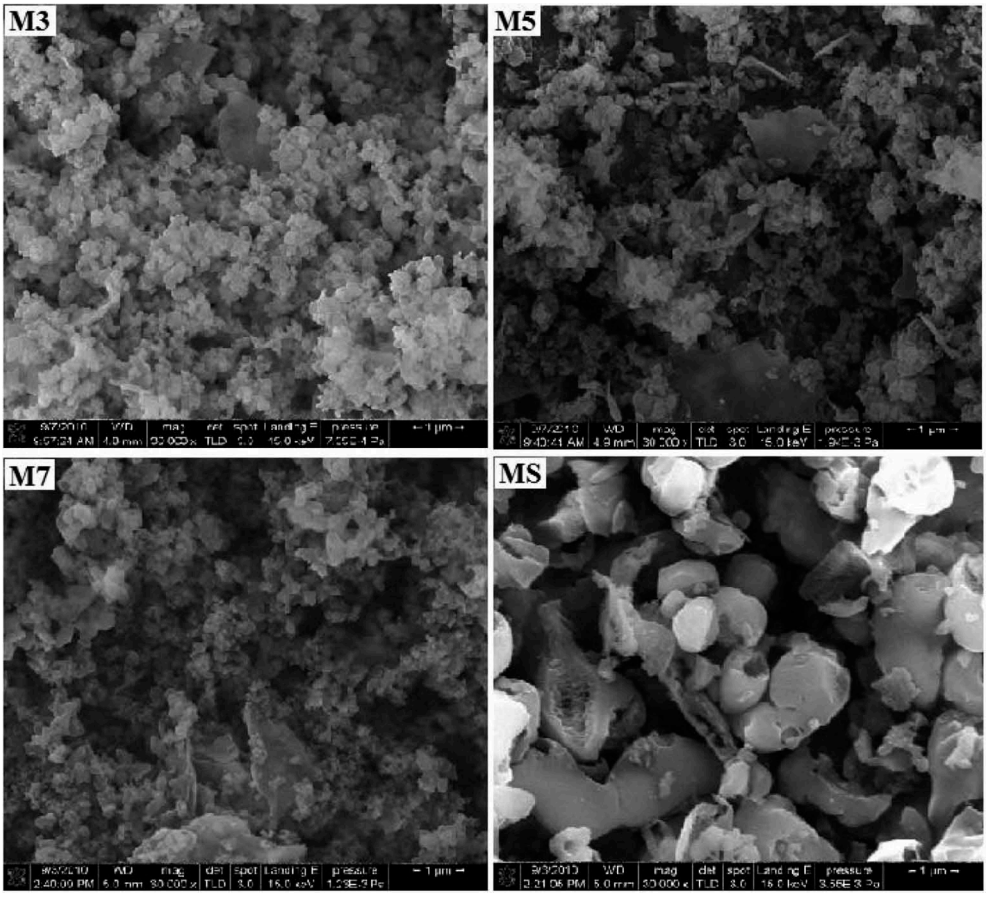

Figure 5. SEM images of MCM-41products.

Moreover, as shown in this figure pore structures are not very prominent and clear. They are almost amorphous in nature. Comparison of the TEM charts between the three samples (M3, M5, and M7) showed the surface of the darkest sample M3, and the inner surface of all the MCM-41 products manufactured from CBA is darker than pure MCM-41 (MS). Although this shows that the highest impurity content found in the sample M3 can be combined with the minimum L/S ratio. By the combination of TEM and SEM evaluation of the composition, the production surface has achieved. As shown in the figure, the dark colour of the surface confirming the appearance of volatile impurities as Mg, Fe, Ca, K, P, S derived from CBA found in mesoporous material obtained.

Figure 7 presents the results obtained from a preliminary analysis of N_2 – adsorption isotherms, which are IV-type in the IUPAC classification with a sharp capillary condensation step at P/Ps = 0,35 designating the uniformity of mesopore. In addition, Figure 8 presents the pore size distributions for the CBA-synthesized MCM-41 and pure silica source MCM-41. Figure 8's results show the sharp and high peak at about 3nm, indicating high homogeneity of mesoporous material obtained from CBA.

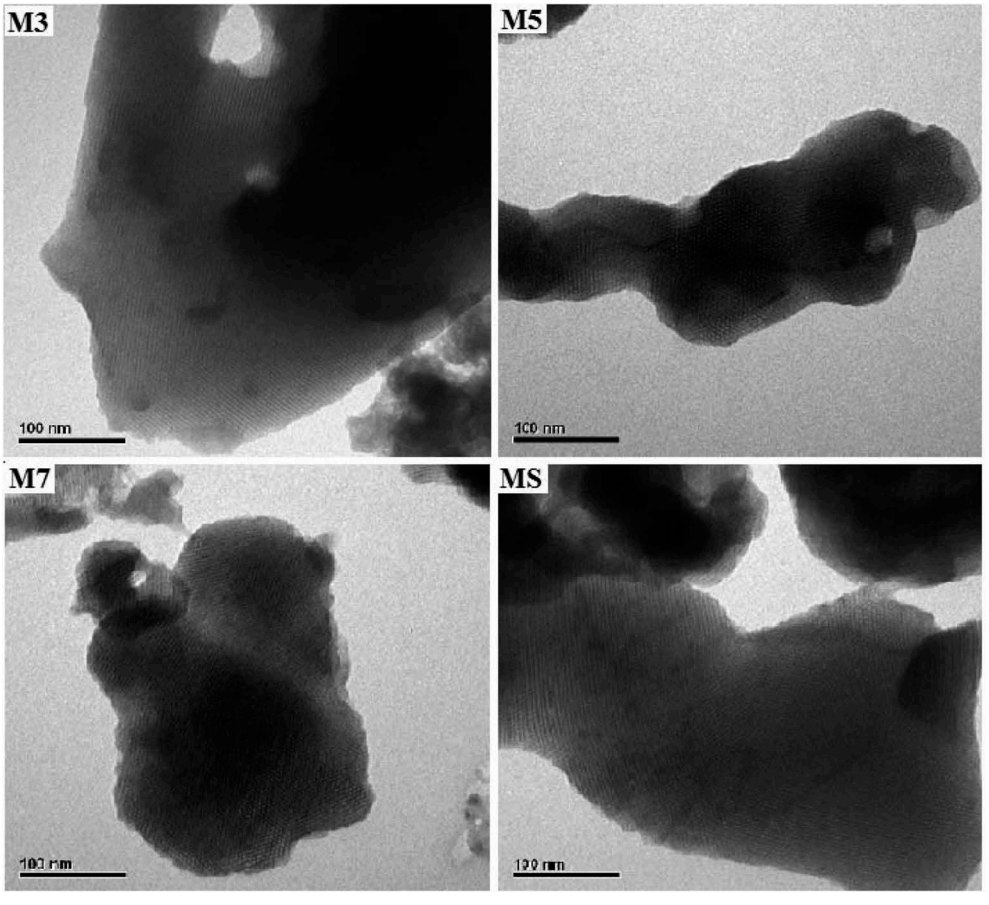

Figure 6. TEM images of MCM-41products.

Table 4 shows the experimental data on the porous characteristics of MCM-41 products. As shown in Table 4, the specific surface area of produced MCM-41 ranged from 796 m^2/g to 932 m^2/g, the total pore volume values and pore diameter were 0.82–0.93 cm^3/g and 3.14–3.22 nm, respectively. The table below indicates a clear trend of the reduced specific surface area of the MCM-41, supposedly due to alkaline conditions in which aluminium was integrated into the silica matrix. The best MCM-41 prepared from CBA according to porous characteristics, was M7 samples. Thus, the total pore volume and the specific surface area of the sample M7 is slightly lower than for samples obtained from pure silica MCM-41 (MS sample). Also, the pore diameter and wall thicknesses are within the MS sample range. The values obtained are similar to MCM-41 manufactured from CFA and Al-MCM-41 from volclay [26].

Figure 9 shows the FTIR spectra of pure silica MCM-41(MS) and CBA -synthesized MCM-41. As can be seen from Figure 9, there were no significant differences between the FTIR result of MS sample and other samples. The bands appearing at of 801.96 cm^{-1} and 1077.9 cm^{-1} correspond to the quartz present or Si-O and Si-O-Si stretching vibrations, respectively. The band of 1629.6 cm^{-1} is corresponding to deformation vibration of adsorbed H_2O or due to C = O groups present in the clay material. The

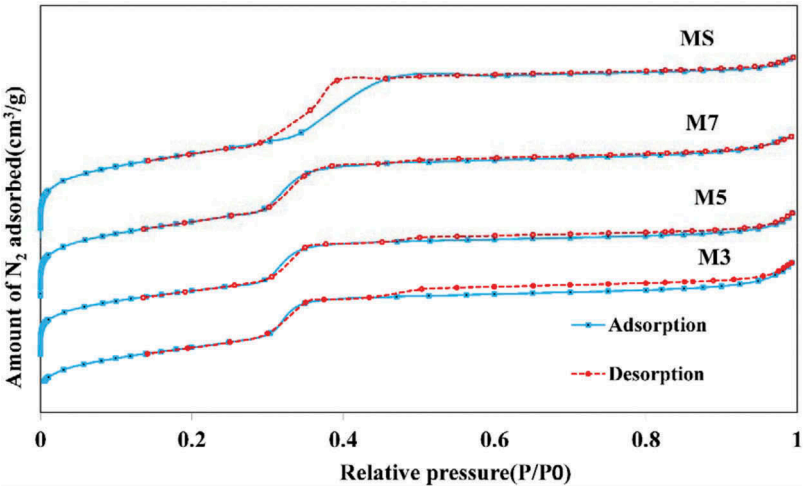

Figure 7. Nitrogen adsorption-desorption results of MCM-41 products.

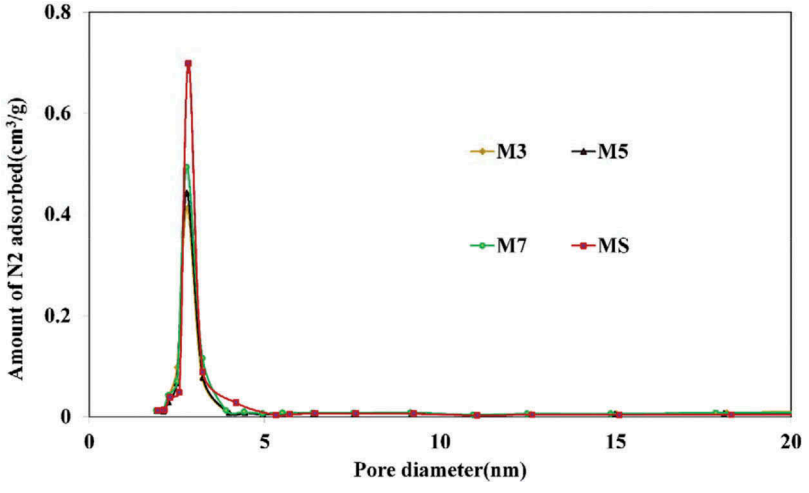

Figure 8. Pore size distribution results of MCM-41products.

Table 4. Porous characteristics of MCM-41 products.

Sample	Specific surface area (m^2/g)	Pore diameter (nm)	Total pore volume (cm^3/g)	d_{100}[a] (nm)	a_o[b] (nm)	W_t[c] (nm)
M3	820	3.22	0.87	3.70	4.27	1.05
M5	796	3.17	0.82	3.75	4.33	1.16
M7	932	3.14	0.93	3.91	4.52	1.38
MS	1047	3.1	1.05	3.66	4.22	1.12

[a] XRD (100) interplanar spacing, [b] Pore diameter, [c] Wall thickness

bands of 2928.9 cm^{-1} and 3415 cm^{-1} are resultant to – CH_2 – symmetric stretching vibration and – OH – stretching vibration, respectively [52]. Finally, the band of 3431.75 cm^{-1} is corresponding to O-H stretching vibration. The FTIR spectrum for

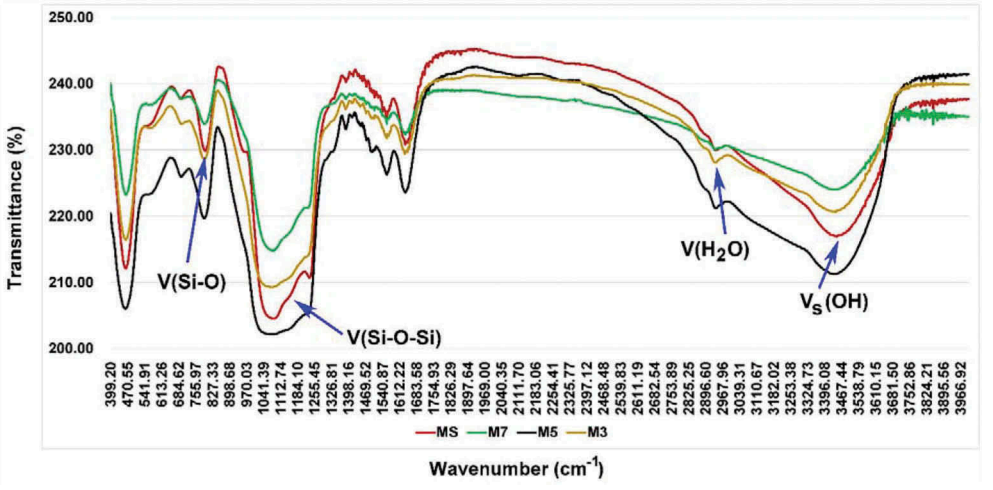

Figure 9. FTIR results of MCM-41products.

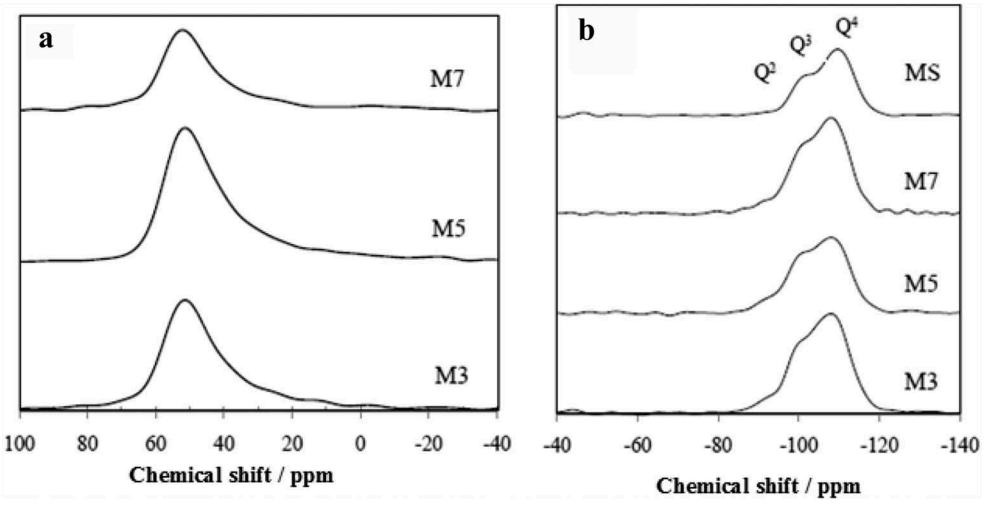

Figure 10. NMR spectrums of MCM-41 products (A – *^{27}Al NMR, B – ^{29}Si NMR*).

CBA-synthesized MCM-41 closely matches with MCM-41 manufactured from CFA and Polish fly ash.

Figure 10 presents the ^{29}Si MAS NMR and ^{27}Al MAS NMR spectra of MCM-41 samples, and they reveal the chemical state of the Si and Al in the framework. Figure 10(a) shows the chemical shift of aluminium in the spectrum representing an intense peak of 50 ppm, indicating that the entire Al was incorporated in tetrahedral coordinates. This is direct evidence of the inclusion of Al in the MCM-41 framework. Figure 10(b) presents the ^{29}Si MAS NMR spectra of MCM-41 samples; the figure shows the occurrence of different oligomeric Si species in the reaction mixture, these species have been identified as Q_i, where i is the number of nearest neighbours Si atoms and has a value of 2–4.

Table 5. The existence percentages of oligomeric Si species (Q_i) in reaction mixtures.

Sample	Q_2(%)	Q_3(%)	Q_4(%)	Q_3/Q_4
M3	8.15	37.45	54.4	0.69
M5	8.66	40.59	50.76	0.79
M7	6.68	38.34	54.98	0.69
MS	3.03	35.74	61.23	0.58

From Figure 10(b) we can see that the highest peak in the spectrum, at −112 ppm concentration, is assigned to the position Q_4 Si had a high polymer [Si (4Si)] and assigned to silica species. The smaller peak at −101 ppm is corresponded to the position Q_3 Si [Si (3Si) OH], while the lowest peak at −90 ppm corresponds to the position Q_2 Si and a sign associated to Si – O – Al [Si (2Si, 2Al)]. These results were also confirmed by the existence percentages of oligomeric Si species in reaction mixtures; they are range from 50.76% to 54.98% of Q_4, from 37.45% to 40.59% of Q_3, and from 6.68% to 8.66% of Q_2 (Table 5). This implies that the merger can be done both dehydrated and soluble silicates and aluminosilicates from CBA. The presence of the species Q_3 and Q_4 demonstrate that a higher degree of silica condensation occurs in the material which is consistent with previous studies.

The selection of the best CBA -synthesized MCM-41 product should satisfy the pure silica source MCM-41. Therefore, based on all the observational features of the MCM-41 products synthesized by CBA, the M7 sample was the most advanced MCM-41 product.

3.3. Adsorption of heavy metal ions

The variation of percentage of metal absorption Pb^{2+}, Cu^{2+} and Cd^{2+} concerning time for two samples CBA-synthesized MCM-41 (M7) and pure silica MCM-41 (MS)

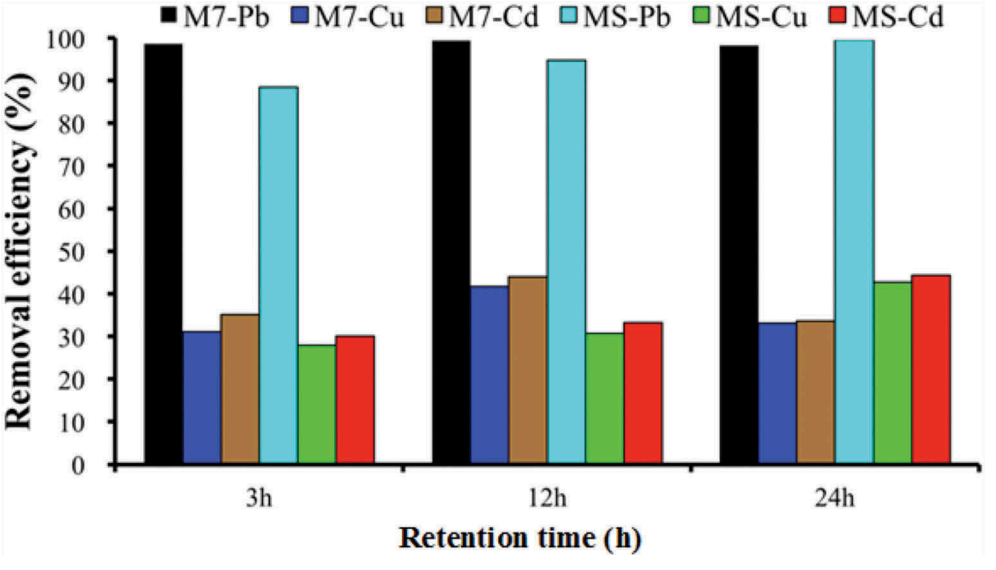

Figure 11. The removal efficiency of Pb^{2+}, Cu^{2+}, and Cd^{2+} in aqueous solution by MCM-41.

was shown in Figure 11. From this Figure, it can be concluded that the greatest effects of M7 in removing Pb^{2+}, Cu^{2+}, and Cd^{2+} from aqueous solutions were 99.4%, 41.66%, and 43.98%, respectively. The experimental results showed that the absorption capacity of samples of M7 and MS for Pb^{2+} metal is higher than Cu^{2+} and Cd^{2+}. The reason is that the hydration radius of Pb^{2+} ions with the value of 0.187nm is smaller than the radius of hydration of Cu^{2+} and Cd^{2+} are 0.210 and 0.215 nm, respectively. With comparing the absorption efficiency of the material over time, it can be seen that the efficiency of the M7 sample with the absorption time of 12 hours (M7-12 h) gives the highest values for all three metals (Pb^{2+}, $Cu^{2+,}$ and Cd^{2+}), and when comparing with the standard MS absorber at 24 hours (MS-24h), the highest values for M7-12 h and MS-24h are 2.55 mmole/g and 2.56 mmole/g, respectively.

As we know, the Freundlich and Langmuir isotherm was most commonly used to define the adsorption of components in solution. They are represented as:

Langmuir isotherm

$$Q_e = \frac{Q_m K_L C_e}{1 + K_L C_e} \tag{1}$$

Freundlich isotherm

$$Q_e = K_F C_e^{\frac{1}{m}} \tag{2}$$

where Q_e and Q_m are the equilibrium adsorption capacity of the adsorbent and the maximum amount of metal sorbed in mg/g, respectively. C_e (mg/l) is the equilibrium concentration of heavy metal ions. The K_L (l/mg) and K_F (mg/l) are the constant that refers to the bonding energy of sorption and the constant related to the adsorption capacity of the adsorbent, respectively. Note that the term *m* was the constant related to the adsorption intensity of the adsorbent [53]. The adsorption isotherms of metal ions by two samples, M7 and MS are shown in Figure 12. The equilibrium adsorption data of Pb^{2+}, Cu^{2+}, and Cd^{2+} ions were fitted into isotherm equations. The experimental data were in good agreement of the Langmuir plots with the suggests a monolayer coverage of metal ions on the outer surface of the adsorbent.

From this figure, the maximum absorbed values (Q_m) for M7-12 h of Pb^{2+}, Cu^{2+} and Cd^{2+} were 204.08 mg/g, 80.05 mg/g and 80.02 mg/g, respectively, whereas these values for of MS-24h were 200.21 mg/g, 78.74 mg/g and 84.03 mg/g, respectively. The maximum adsorption capacity was observed for Pb^{2+} due to the physicochemical properties of Pb^{2+}, having higher atomic weight, electrode potential, electronegativity, and larger ion size than Cu^{2+} and Cd^{2+}. For all cases, the Freundlich model represents a better fit to the experimental data than the Langmuir model. In addition, the values of Langmuir, including Q_m, b and Freundlich parameters K and 1/m, are listed in Table 6. The obtained results show that the R^2 value is always greater than 0.90 for both models and the value of 1/m is less than 1 for all different materials, indicating high adsorption capacity of the sample M7 [20]. The Langmuir isothermal model indicates that the K_L value of ion Pb^{2+} is higher than that of Cu^{2+} and Cd^{2+} ions, designating that the adsorption ability of ion Pb^{2+} is higher than that of Cu^{2+} and Cd^{2+} ions [54].

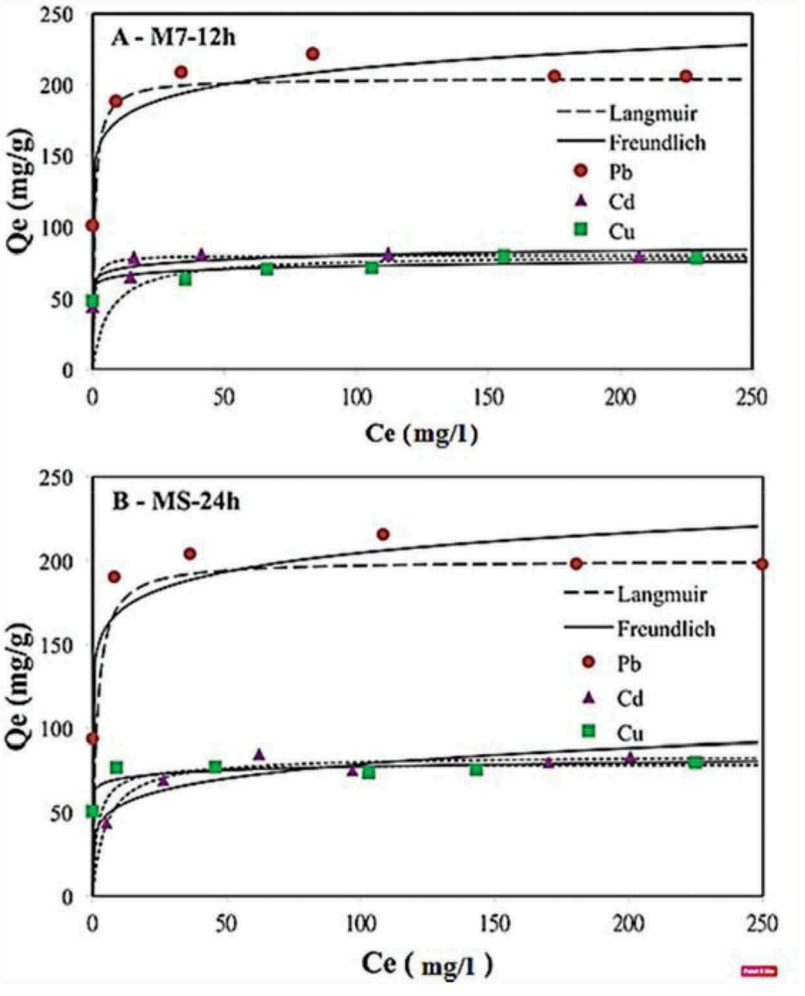

Figure 12. The isotherm fits for the data of Pb^{2+}, Cu^{2+}, and Cd^{2+} sorption, A for M7-12 h sample and B for MS-24 h sample.

Table 6. Parameters of isotherms fit of adsorption data.

		Langmuir model			*Freundlich model*		
Samples	Metals	Q_m(mg/g)	K_L(l/mg)	R^2	1/m	K_F(l/mg)	R^2
M7-12 h	Pb^{2+}	204.08	1.98	0.9993	0.08	145.20	0.9274
	Cd^{2+}	80.02	1.17	0.9995	0.05	62.43	0.9227
	Cu^{2+}	80.05	0.15	0.9962	0.05	58.83	0.9048
MS-24 h	Pb^{2+}	200.21	0.66	0.9987	0.08	140.58	0.9031
	Cd^{2+}	84.03	0.20	0.9968	0.07	36.73	0.8331
	Cu^{2+}	78.74	0.52	0.9981	0.04	63.30	0.8961

To sum up, the metal adsorption capacity of previous studies was compared with present work. Table 7 lists the values of the absorption capacity of metal ions by different adsorbents. The maximum value of Pb^{2+} absorption is 117.51 mg/g [55] while the absorption capacity of this study is 204.08 mg/g. The highest Cu^{2+}

Table 7. Comparing research results with previous studies.

Adsorbents	Specific surface area (m^2/g)	Metals (Q_m, mg/g)			References
		Pb^{2+}	Cu^{2+}	Cd^{2+}	
Activated carbon	253	-	40	15	[56]
Activated carbon	550	-	-	16.7	[58]
Activated carbon	472	64.1	30.7	-	[59]
NH_2-MCM-41	750	-	-	79.8	[57]
NH_2-MCM-41	966	57.74	-	18.25	[54]
Al-GPTS-KOBut-H	-	78.8	76.5	-	[60]
MCM41-BA	992	34.2	9	17.1	[61]
MCM-41	932	***204.08***	***80.05***	***80.02***	***Current study***

absorption equivalent to 40 mg/g [56] while the value of this study is 80.02 mg/g. The maximum absorption value of Cd^{2+} is 79.8 mg/g [57] while the absorption capacity of Cd^{2+} of this study is 80.05 mg/g. From the above comparison, it can be concluded that the ability to absorb heavy metal from bottom ash is very good.

4. Conclusion

This research has studied the feasibility of synthesizing mesoporous molecular sieve (MCM-41) through alkaline-hydrothermal treatment using coal bottom ash. The synthesized characteristics are similar to the MCM-41 produced by a standard method using pure silica sources. The results indicate that a NaOH/CBA ratio and heating temperature were the significant factors to determine optimal conditions for alkaline fusion. The L/S ratio for deionized water and the filtered solid influenced the ratio of Si/Al in the precursor solution. The XRD consequence of the CBA -synthesized MCM-41 shows that the high orderly structure was attained and that the mesoporous normal hexagonal structure of the MCM-41 was typically retained after removal of the surfactant. The best CBA-synthesized MCM-41 had a uniform pore size, a pore diameter of 3.14 nm, a BET surface area of 932 m^2/g and a pore volume of 0.93 cm^3/g as well as comparing with the common values announced for pure silica MCM-41 with conventional synthesis. This result suggests that coal bottom ash could be a potential, environmentally friendly and economic silica source in the manufacturing of MCM-41 materials. Metal ion absorption (Pb^{2+}, Cu^{2+}, and Cd^{2+}) was tested for the best MCM-41 product. The results show that the adsorption equilibrium of product was achieved in 12 hours with the value of 204.08 mg/g, 80.05 mg/g and 80.02 mg/g for Pb^{2+}, Cu^{2+}, and Cd^{2+}, respectively, at the temperature of 25°C, pH value of 5. Data absorption equilibrium is very suitable for Langmuir and Freundlich adsorption models. Our current study reveals that synthesized adsorbent as an effective and recyclable adsorbent has a high potential to remove heavy metals in wastewater.

Briefly, it can be said that:

(1) Coal Fly ash as a cheap silica source can be used for the synthesis of mesoporous materials.
(2) The maximum adsorption capacity of heavy metals onto mesoporous MCM-41material could be up to 204.08 mg/g.
(3) The adsorption of ability of ion Pb^{2+} is higher than that of Cu^{2+} and Cd^{2+} ions in aqueous solution by MCM-41.

(4) The main disadvantage of MCM-41 is the lack of effective binding groups which need modification of the MCM-41 surface with several groups.

Author Contributions

Data collection and experimental works: Dinh-Hieu Vu, Qui-Thao Le, Dinh-An Nguyen, Ngoc-Hoan Do
Writing, discussion, analysis: Dinh-Hieu Vu, Hoang-Bac Bui, Xuan-Nam Bui, Hoang Nguyen

Disclosure statement

No potential conflict of interest was reported by the authors.

Funding

This work was funded by National Foundation for Science and Technology Development (NAFOSTED) in Vietnam under grant number 105.08-2014.10.

ORCID

Xuan-Nam Bui http://orcid.org/0000-0001-5953-4902
Hoang Nguyen http://orcid.org/0000-0001-6122-8314

References

[1] M. Kalaw, A. Culaba, H. Hinode, W. Kurniawan, S. Gallardo and M. Promentilla, Materials **9**, 580 (2016). doi:10.3390/ma9070580.
[2] B. Valentim, et al., Minerals. **8**, 140 (2018). doi:10.3390/min8040140
[3] H. Kim, J.W. Choi, T.H. Kim, J.S. Park and B. An, Water **10**, 1069 (2018). doi:10.3390/w10081069.
[4] N.A. Rashidi, S. Yusup and A.C.S. Sustain, Chem. Eng. **4**, 1870 (2016). doi:10.1021/acssuschemeng.5b01437.
[5] D.H. Vu, K.-S. Wang and B.H. Bac, Mater. Lett. **65**, 940 (2011). doi:10.1016/j.matlet.2011.01.006.
[6] Y. Xiao, J. Yin, Y. Hu, J. Wang, H. Yin and H. Qi, Sustainability **11**, 217 (2019). doi:10.3390/su11010217.
[7] S.C. Pan, C.C. Lin and D.H. Tseng, Resour. Conserv. Recycl. **39**, 79 (2003). doi:10.3390/su11010217.
[8] J. Ge, S. Yoon and N. Choi, Appl. Sci. **8**, 1116 (2018). doi:10.3390/app8071116.
[9] I. Fonts, M. Azuara, G. Gea and M.B. Murillo, J. Anal. Appl. Pyrolysis. **85**, 184 (2009). doi:10.1016/j.jaap.2008.11.003.
[10] B. Khiari and M. Jeguirim, Energies **11**, 730 (2018). doi:10.3390/en11040730.
[11] K.L. Lin, W.C. Chang, D.F. Lin, H.L. Luo and M.C. Tsai, J. Environ. Manage. **88**, 708 (2008). doi:10.1016/j.jenvman.2007.03.036.
[12] L. Tambara Júnior, M. Cheriaf and J. Rocha, Materials **11**, 1829 (2018). doi:10.3390/ma11101829.
[13] W.T. Kuo and Z.C. Gao, Appl. Sci. **8**, 1377 (2018). doi:10.3390/app8081377.
[14] C.R. Cheeseman and G.S. Virdi, Resour. Conserv. Recycl. **45**, 18 (2005). doi:10.1016/j.resconrec.2004.12.006.
[15] H. Misran, R. Singh, S. Begum and M.A. Yarmo, J. Mater. Process. Technol. **186**, 8 (2007). doi:10.1016/j.jmatprotec.2006.10.032.

[16] K. Czarnobaj, M. Prokopowicz and K. Greber, Int. J. Mol. Sci. **20**, 1311 (2019). doi:10.3390/ijms20061311.
[17] R. Qi, et al, Sens. Actuators B Chem. **277**, 584 (2018). doi:10.1016/j.snb.2018.09.062
[18] S. Kunchakara, M. Dutt, A. Ratan, J. Shah, V. Singh and R.K. Kotnala, J. Porous Mater. **1** (2018). doi:10.1007/s1093
[19] D. Chen, H. Zeng, C. Cen, Z. Chen and Z. Tang, DEStech Trans. Eng. Technol. Res. 2018. doi:10.12783/dtetr/icace2018/25557
[20] A. Benhamou, M. Baudu, Z. Derriche and J.P. Basly, J. Hazard. Mater. **171**, 1001 (2009). doi:10.1016/j.jhazmat.2009.06.106.
[21] J. Cecilia, C. García-Sancho, C. Jiménez-Gómez, R. Moreno-Tost and P. Maireles-Torres, Materials **11**, 1569 (2018). doi:10.3390/ma11091569.
[22] F. Ramírez Rodríguez, L. Giraldo and B. Lopez, C **4**, 16 (2018). doi:10.3390/c4010016.
[23] A. Al-Fatesh, et al., Catalysts. **8**, 229 (2018). doi:10.3390/catal8060229
[24] K.S. Hui and C.Y.H. Chao, J. Hazard. Mater. **137**, 1135 (2006). doi:10.1016/j.jhazmat.2006.03.050.
[25] R.V. Sales, et al., Adsorption. **1** (2019). doi:10.1007/s10450-019-00088-4
[26] M. Adjdir, T. Ali-Dahmane, F. Friedrich, T. Scherer and P.G. Weidler, Appl. Clay Sci. **46**, 185 (2009). doi:10.1016/j.clay.2008.11.009.
[27] M. Adjdir, et al., C. R. Chim. **18**, 385 (2015). doi:10.1016/j.crci.2014.07.003
[28] P. Mohanty, et al., Micropor. Mesopor. Mater. **152**, 214 (2012). doi:10.1016/j.micromeso.2011.11.031
[29] V. Stagno, et al., **187**, 145 (2014). doi:10.1016/j.micromeso.2013.12.032
[30] V. Stagno, M. Mandal, K. Landskron and Y. Fei, Phys. Chem. Miner. **42**, 509 (2015). doi:10.1007/s00269-015-0739-8.
[31] L. Zhang, P. Mohanty, N. Coombs, Y. Fei, H.-K. Mao and K. Landskron, Proc. Natl. Acad. Sci. **107**, 13593 (2010). doi:10.1073/pnas.1006938107.
[32] I. Majchrzak-Kucęba and W. Nowak, Int. J. Miner. Process. **101**, 100 (2011). doi:10.1016/j.minpro.2011.09.002.
[33] M. Kadhom, J. Yin and B. Deng, Membranes **6**, 50 (2016). doi:10.3390/membranes6040050.
[34] M. Mokhter, et al., Colloid. Interfac. **2**, 19 (2018). doi:10.3390/colloids2020019
[35] M. Kragović, et al., Minerals. **8**, 11 (2018). doi:10.3390/min8010011
[36] C. El Abiad, S. Radi, M.A.F. Faustino, M. Neves and N.M.M. Moura, Molecules **24**, 669 (2019). doi:10.3390/molecules24040669.
[37] S. Babel and T.A. Kurniawan, J. Hazard. Mater. **97**, 219 (2003). doi:10.1016/S0304-3894(02)00263-7.
[38] F. Fu and Q. Wang, J. Environ. Manage. **92**, 407 (2011). doi:10.1016/j.jenvman.2010.11.011.
[39] P.A. Mangrulkar, S.P. Kamble, J. Meshram and S.S. Rayalu, J. Hazard. Mater. **160**, 414 (2008). doi:10.1016/j.jhazmat.2008.03.013.
[40] K.A. Northcott, K. Miyakawa, S. Oshima, Y. Komatsu, J.M. Perera and G.W. Stevens, Chem. Eng. J. **157**, 25 (2010). doi:10.1016/j.cej.2009.10.038.
[41] M. Algarra, M.V. Jiménez, E. Rodríguez-Castellón, A. Jiménez-López and J. Jiménez-Jiménez, Chemosphere **59**, 779 (2005). doi:10.1016/j.chemosphere.2004.11.023.
[42] C. Cai, H. Wang and J. Han, Appl. Surf. Sci. **257**, 9802 (2011). doi:10.1016/j.apsusc.2011.06.025.
[43] D. Pérez-Quintanilla, I. Del Hierro, M. Fajardo and I. Sierra, Micropor. Mesopor. Mater. **89**, 58 (2006). doi:10.1016/j.micromeso.2005.10.012.
[44] Q. Qin, J. Ma and K. Liu, J. Hazard. Mater. **162**, 133 (2009). doi:10.1016/j.jhazmat.2008.05.016.
[45] X. Wang, Y. Jin, Z. Wang, Y. Nie, Q. Huang and Q. Wang, Waste Manag. **29**, 1330 (2009). doi:10.1016/j.wasman.2008.09.006.
[46] R. Ryoo and J.M. Kim, J. Chem. Soc. Chem. Commun. **711** (1995). doi:10.1039/C39950000711
[47] D.H. Vu, K.S. Wang, B.X. Nam, B.H. Bac and T.C. Chu, Ceram. Int. **37**, 2845 (2011). doi:10.1016/j.ceramint.2011.04.118.
[48] M. Erol, S. Küçükbayrak and A. Ersoy-Meriçboyu, J. Hazard. Mater. **153**, 418 (2008). doi:10.1016/j.jhazmat.2007.08.071.

[49] X. Chen, S. Zhou, L. Zhang, T. You and F. Xu, Materials **9**, 582 (2016). doi:10.3390/ma9070582.
[50] M. Wang, Z. Wang, X. Zhou and S. Li, Appl. Sci. **9**, 547 (2019). doi:10.3390/app9030547.
[51] E. Manaila, G. Craciun, D. Ighigeanu, C. Cimpeanu, C. Barna and V. Fugaru, Materials (Basel) **10**, 540 (2017). doi:10.3390/ma10050540.
[52] A. Kayan, J. Inorg. Organomet. Polym. Mater. **25**, 1345 (2015). doi:10.1007/s10904-015-0246-x.
[53] L. Zhang, et al., J. Chem. Eng. Data. **64**, 176 (2019). doi:10.1021/acs.jced.8b00689
[54] A. Heidari, H. Younesi and Z. Mehraban, Chem. Eng. J. **153**, 70 (2009). doi:10.1016/j.cej.2009.06.016.
[55] X. Liang, Y. Xu, G. Sun, L. Wang, Y. Sun and X. Qin, Colloid. Surf. A Physicochem. Eng. Asp. **349**, 61 (2009). doi:10.1016/j.colsurfa.2009.07.052.
[56] M.J. Martin, A. Artola, M.D. Balaguer, M. Rigola and J. Chem, Technol. Biotechnol. Int. Res. Process. Environ. Clean Technol. **77**, 825 (2002). doi:10.1002/jctb.645.
[57] K.F. Lam, K.L. Yeung and G. McKay, Environ. Sci. Technol. **41**, 3329 (2007). doi:10.1021/es062370e.
[58] Y. Zhai, X. Wei, G. Zeng, D. Zhang and K. Chu, Sep. Purif. Technol. **38**, 191 (2004). doi:10.1016/j.seppur.2003.11.007.
[59] F. Rozada, M. Otero, A. Morán and A.I. García, Bioresour. Technol. **99**, 6332 (2008). doi:10.1016/j.biortech.2007.12.015.
[60] E. Cerrahoğlu, A. Kayan and D. Bingöl, Sep. Sci. Technol. **53**, 2563 (2018). doi:10.1080/01496395.2018.1465979.
[61] Z.-S. Liu, W.K. Li and C.Y. Huang, Waste Manag. **34**, 893 (2014). doi:10.1016/j.wasman.2014.02.016.